

On the origin of continuum and line emission in CTTSs

S. A. Lamzin¹, M. M. Romanova² and A. S. Kravtsova¹

¹Sternberg Astronomical Institute, Universitetskij prospect 13, Moscow, 119991, Russia
email: lamzin@sai.msu.ru, kravts@sai.msu.ru

²Department of Astronomy, Cornell University, Ithaca, NY 14853-6801, USA
email: romanova@astro.cornell.edu

Abstract. We calculated profiles of CIV 1550Å, Si IV 1400Å, NV 1240Å and OVI 1035Å doublet lines using results of 3D MHD simulations of disc accretion onto young stars with a dipole magnetic field. It appeared that our calculations cannot reproduce the profiles of these lines observed (HST/GHRS-STIS and FUSE) in CTTSs spectra. We also found that the theory predicts much larger CIV 1550Å line flux than observed (up to two orders of magnitude in some cases) and argue that the main portion of accretion energy in CTTSs is liberated outside the accretion shock. We conclude that the reason of disagreement between the theory and observation is the strongly non-dipolar character of CTTS magnetic field near its surface.

Keywords. Stars: pre-main-sequence, shock waves, ultraviolet: stars, magnetic fields.

1. Introduction

Since the beginning of the 1990s, there has been a consensus that the line and continuum emission observed in the spectra of classical T Tauri stars (CTTSs) results from the magnetospheric accretion of circumstellar material. More precisely, the magnetic field of the star is believed to stop the accretion disk from reaching the stellar surface. In some way the disk material becomes frozen in the magnetospheric field lines and slides along them toward the stellar surface, eventually being accelerated to velocities $V_0 \sim 300$ km/s. The gas is then decelerated in an accretion shock, whose radiation presumably gives rise to the observed line and continuum emission.

The radial extension of pre- and post-shock radiating regions of CTTS accretion shock is much smaller than the stellar radius – $Z_{pre}, Z_{pst} \ll R_*$ in Figure 1, – making it possible to calculate the structure and spectrum of the accretion shock in the 1-D approximation (Lamzin 1995). Calculations of Lamzin (1998) and Calvet & Gullbring (1998) indicated that the structure of the flow can be specified nearly unambiguously by two parameters: the velocity V_0 and density ρ_0 (or particle number density N_0) of the gas far in front of the shock.

Calvet & Gullbring (1998) used results of their calculations to derive the parameters of the accretion shock via modeling of the continuum spectral energy distributions of classical T Tauri stars. However, they did not take into account limb darkening effects. Furthermore, the agreement between the calculated and observed spectra of the veiling continuum cannot be considered as a decisive support for the magnetospheric model, since boundary-layer models provide equally good agreement – see e.g. Basri & Bertout (1989). The line spectrum is far more informative, and comparisons of the calculated and observed intensities and profiles of emission lines enable detailed studies of the accretion processes.

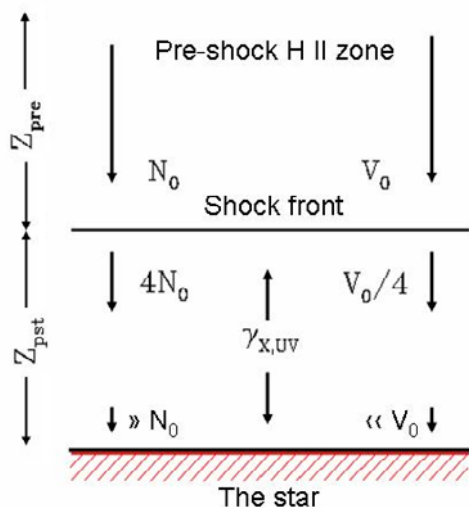


Figure 1. Schematic structure of CTTS accretion shock.

Optically thin lines are best suited for this purpose: their intensity ratios can be used to derive physical conditions independent of the geometry of the region where they are formed, and the line profiles provide information about both the velocity field and the geometry of this region. Calculations by Lamzin & Gomez de Castro (1999) demonstrated that the O III] 1663Å, Si III] 1892Å and C III] 1909Å lines should display the highest intensities among the optically thin lines, and these lines were used to determine the accretion-shock parameters for several young stars in that paper. However, Gomez de Castro & Verdugo (2001, 2007) questioned whether these lines form in the accretion shock. Spectral lines of neutral or singly ionized atoms apparently form not only in the accretion shock but in the magnetospheric flow and wind as well – see e.g. Edwards, this volume – and thus likewise cannot be used as diagnostics of the accretion shock.

Resonant UV lines of the C IV, Si IV, NV and O VI uv1 doublets look as the most suitable diagnostics of CTTSs accretion shock, especially lines of the C IV 1550Å doublet: they are strong in CTTS spectra and the calculation of their intensities is relatively simple.

2. Intensities of the C IV 1550Å doublet lines: theory vs. observations

Generally speaking, lines of C^{+3} , Si^{+3} , N^{+4} and O^{+5} ions form before and behind the shock front. Gas temperature in the pre-shock (precursor) zone of CTTSs does not exceed 20,000 K, but ions up to O^{+5} (at $200 < V_0 < 400$ km/s) exist here due to the photoionization of accreted matter by X-ray and UV quanta from the post-shock cooling zone. When infalling gas crosses the shock front its temperature raises up to 1-3 MK and for example C^{+3} ions almost completely transform to C^{+6} ions. Then the gas cools down and ions of interest appear again but at a gas velocity close to zero – see Lamzin (1998) for details.

Lamzin (2003a) carried out non-LTE calculations of profiles of C IV 1550Å, Si IV 1400Å, NV 1240Å and O VI 1035Å doublet lines for a plane-parallel shock viewed at various angles. Calculations were performed for a range of preshock gas parameters V_0 , N_0 appropriate for CTTSs. Intensities of C IV 1548+1551Å lines, normalized to $\mathcal{F} = \rho_0 V_0^4/4$, as a function of cosine μ of the angle between the normal to the shock front and the line

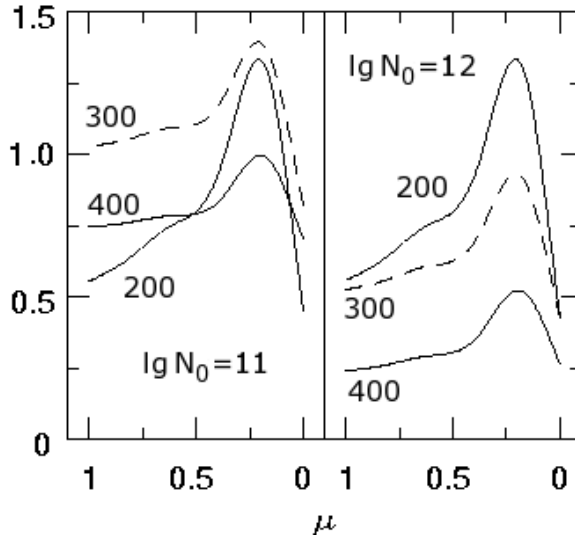


Figure 2. Relative intensities of the CIV 1550Å doublet lines expressed in percent. See text for details.

of sight are presented in Figure 2. The ratio is expressed in percent, such as different lines in the figure correspond to different infall gas velocities ($V_0 = 200, 300$ and 400 km/s). The results were calculated for a gas particle density of $N_0 = 10^{11}$ cm $^{-3}$ (left panel) and 10^{12} cm $^{-3}$ (right panel).

The value \mathcal{F} was chosen for normalisation because this value is expected to be equal to the bolometric flux of the veiling continuum emission produced by the accretion shock. Indeed, according to the current paradigm half of the X-ray and UV quanta from the post-shock cooling zone reach the stellar surface. These quanta are absorbed in the upper layers of the stellar atmosphere and then should be predominantly reradiated in the continuum – see Calvet & Gullbring (1998) for details. Thus the ratio δ , depicted in Figure 2, is the theoretical prediction for the ratio of CIV 1550Å doublet line flux to the bolometric flux of the veiling continuum. Thus this ratio is expected to be $\simeq 1\%$ and almost independent of V_0 and N_0 .

Meanwhile it was found that the observed ratio is much smaller – see Table 1 in which we summarised the results of our analysis of CTTs UV spectra observed by the Hubble Space Telescope (Kravtsova & Lamzin 2002a; Kravtsova & Lamzin 2002b; Kravtsova 2003; Lamzin *et al.* 2004). The discrepancy between theory and observation is significant – more than two orders of magnitude in the case of RY Tau and DR Tau, such as this conclusion does not depend on current uncertainty on the value and law of interstellar extinction in the direction of the investigated stars.

Table 1. Relative contribution of CIV lines to the emission of accretion shock

Star:	RY Tau	DR Tau	T Tau	DS Tau	BP Tau	DG Tau	Theory
$\delta, \%$	0.002	0.003	0.02	0.02	0.04	0.07	~ 1.0

We suppose that this discrepancy means that the main portion of the veiling continuum (up to 99 % in some cases judging from Table 1) originates outside the CIV 1550Å line formation region, i.e., outside the *strong* (Mach number $M_{sh} \gg 1$) accretion shock. In other words, we conclude that the main portion of the accreted matter does not pass

through the accretion shock and falls to the star almost parallel to the stellar surface. In this part of the accretion flow the conversion of the kinetic energy of the infalling gas into heat and then into radiation should occur in the same way(s) as in a boundary layer, i.e., in a series of *weak* ($M_{sh} \simeq 1$) oblique shocks. One can estimate the maximum possible angle γ_{sh} between the front of weak oblique shocks and the stellar surface as follows.

In the coronal equilibrium approximation C^{+3} ions forms at $T \simeq 10^5$ K. Such a temperature can be reached immediately behind the shock front if the accreted gas velocity component V_r normal to stellar surface is $\simeq 70$ km/s. Therefore oblique accretion shocks with V_r less than this value cannot contribute to the CIV 1550Å line emission of the accretion flow but produce veiling continuum and emission of neutral lines, and of singly or twice ionized atoms. If the typical infall gas velocity V_0 is $\simeq 300$ km/s, then $\gamma_{sh} = \sin^{-1}(V_r/V_0) < 15^\circ$, i.e. gas producing such weak shocks indeed falls onto the star almost parallel to its surface.

3. Profiles of CIV 1550Å doublet lines: theory vs. observations

As was mentioned above the CIV 1550Å doublet lines form in two spatially distinct regions of strong accretion shock: in the radiative precursor and in the post-shock zone. Gas velocity in these regions are different: $V \simeq V_0 \sim 300$ km/s in the pre-shock zone and $\sim 5 - 10$ km/s in the post-shock line formation region. As a result the profile of e.g. the CIV 1548Å line in the spectrum of a plane-parallel shock, viewed from the direction perpendicular to the surface of the shock front, should have two components: the first one is at almost zero-velocity and the second is redshifted to V_0 . As follows from our calculations (Lamzin 2003a), both components are optically thick, resulting in a FWHM for each component of $\sim 20 - 30$ km/s, with a relative strength depending on V_0 : at $V_0 < 300$ km/s the “zero-velocity” component is stronger than the “high-velocity” one and vice versa at $V_0 > 300$ km/s. If the shock is viewed from a direction that makes an angle θ with the perpendicular to the shock surface, then the “zero-velocity” component should be seen practically at the same position but the redshifted “high-velocity” peak should now be at $V_0 \mu$, where $\mu = \cos \theta$. The same is true (in a qualitative way) for lines of Si IV 1400Å, NV 1240Å and OVI 1035Å doublets.

Consider now a part of CTTS surface occupied with strong accretion shock (accretion zone). The observed profile of e.g. the CIV 1548Å line emitted by the accretion shock is the sum (an integral) of the double-peaked profiles from all elementary areas ΔS of the accretion zone (multiplied by the $\mu \Delta S$ factor). All elementary areas are viewed at different angles due to the curvature of stellar surface and these angles vary with time due to stellar rotation. One can expect that the intensities of “zero-velocity” components from all parts of the accretion zone will sum up and the (weighted) sum of high-velocity components will result in a more or less wide red wing or separated redshifted component depending on the distribution of V_0 and N_0 in the accretion zone and on its geometry. Obviously the profile should vary with time due to stellar rotation and non-stationary accretion as well.

Lamzin (2003b) calculated the profiles of the CIV 1550Å doublet lines from a strong accretion shock assuming that: 1) matter falls to the star in the radial direction; 2) V_0 and N_0 are constant within the accretion zone; 3) the zone has the shape of a circular spot or a spherical belt. The results of the calculations were compared to the profiles of UV lines in the spectra of CTTSs observed with the Goddard High Resolution Spectrograph (GHRS) and Space Telescope Imaging Spectrograph (STIS). Observational data were extracted from the scientific archives of the HST. The calculated profiles differ significantly from the

observed ones presumably because our assumptions about the character of the accretion flow near the stellar surface were not realistic enough.

One can expect better agreement by using parameters of an accretion flow derived from 3D MHD simulations of disc accretion to a slowly rotating magnetized young star with its dipole moment inclined at an angle α to the stellar rotation axis. Accretion rate \dot{M}_{acc} , polar magnetic field strength B as well as mass and radius of the central star are free parameters of these simulations in addition to the angle $0 \leq \alpha \leq 90^\circ$ – see Romanova *et al.* (2003) for details. The velocity field \mathbf{V}_0 and gas density ρ_0 at the stellar surface, adopted from the simulations, were used as input parameters to calculate profiles of CIV 1550Å, Si IV 1400Å, NV 1240Å and OVI 1035Å doublet lines. For all models we adopted $M_* = 0.8 M_\odot$, $R_* = 1.8 R_\odot$, $B = 1 - 3$ kG and varied α , \dot{M}_{acc} in the $0^\circ - 90^\circ$ and $10^{-8} - 3 \cdot 10^{-7} M_\odot/\text{yr}$ intervals respectively. Profiles were calculated for each accretion zone model with different values of the angle between the stellar rotation axis and the line of sight ($0^\circ \leq i \leq 90^\circ$) as well as for a set of phases of stellar rotation periods, i.e., for different angles ψ (in 2π units) between the magnetic dipole axis and the plane which contains the rotation axis and the line of sight ($0 \leq \psi \leq 1$).

Observed profiles of the CIV 1550Å doublet lines in DS Tau, BP Tau, DF Tau and DR Tau spectra are shown in Figure 3. Solid and dashed lines depicts CIV 1548Å and CIV 1551Å components of the doublet. Profiles of the CIV 1550Å doublet components in the spectrum of T Tau are shown in Figure 4 (left column). T Tau is the only star where there is more than one high resolution UV spectrum and one can observe variability of the CIV doublet lines profiles. Only in the case of TW Hya (right panel of the figure) is there a possibility to obtain information about lines of the OVI 1035Å doublet – see Ardila, this volume for references and details.

We plot in Figure 5 the results of our calculations for the model with $\alpha = 30^\circ$, $\dot{M}_{acc} \simeq 4 \cdot 10^{-8} M_\odot/\text{yr}$, $i = 10^\circ$ (left panel) and $i = 70^\circ$ (right panel). The vertical row of profiles in each panel corresponds to the following set of rotational phases (from top to bottom): $\psi = 0, 0.25, 0.5, 0.75$. Profiles were normalized to the maximum intensity of the line at

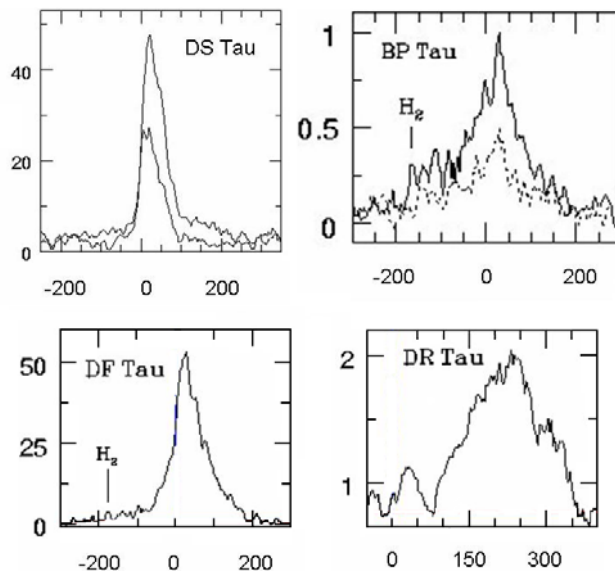


Figure 3. Profiles of the CIV 1550Å doublet lines in the spectra of some CTTSs.

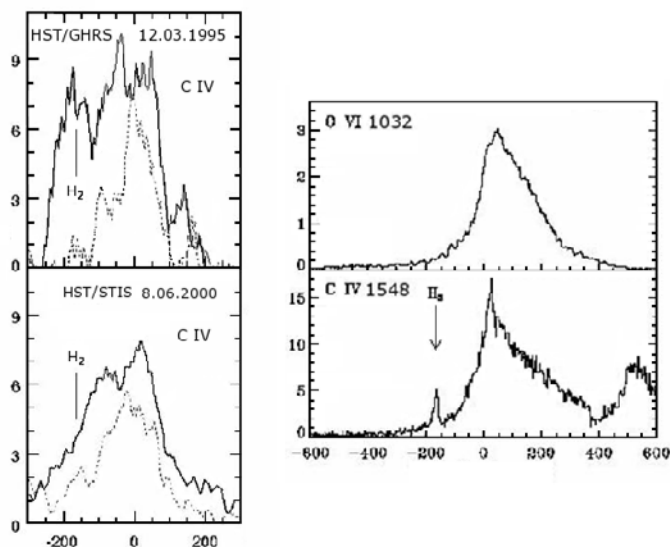


Figure 4. Profiles of the C IV 1550Å and O VI 1035Å doublet components in the spectra of T Tau (left panel) and TW Hya (right panel).

$\psi = 0$. It was assumed that the accretion disk does not prevent to observe the part of the star that is situated below the disk midplane – this is the reason why some profiles have an extended blue wing.

Matter falls to the star with a dipole magnetic field at an angle $\theta < 90^\circ$ relative to its surface. In the absence of a magnetic field oblique shocks would arise, which means that: 1) the shock front is parallel to the stellar surface; 2) the velocity component V_r which is parallel to stellar radius is at the pre-shock velocity V_0 . But bear in mind that since the accreted gas moves along the magnetic field lines it also seems reasonable to suppose that the shock front is perpendicular to the magnetic field lines and therefore $V_0 = V$. We calculated line profiles for both cases: solid lines in Figure 5 correspond to profiles calculated for the $V_0 = V_r$ case and dashed lines for the $V_0 = V$ case.

Such an approach looks reasonable at the moment as both types of theoretical profiles differ from the profiles of the C IV 1548Å line observed in spectra of CTTS shown in Figures 3, 4. Observed profiles have only one peak at nearly zero velocity position. The only exception is DR Tau: the profile its C IV 1548Å line consists of two redshifted components but the intensity of the “high-velocity” component is larger than that of the “low-velocity” one. Theoretical profiles calculated for models with other values of α , \dot{M}_{acc} and i have qualitatively the same shape as those shown in Figure 5, i.e., cannot reproduce observations either.

We suppose that the reason of the discrepancy is the small spread of the accreted gas stream lines within accretion zone which occupies only $\sim 5\%$ of the stellar surface (Romanova *et al.* 2003). Would the spread of the stream (and therefore of the magnetic field) lines within the accretion zone be larger, it would seem possible to obtain single-peak profiles with an extended red wing similar to the observed ones. In any case our results indicate that the magnetic field of CTTSs is significantly non-dipolar near the stellar surface in agreement with direct magnetic field measurements (see Johns-Krull, this volume).

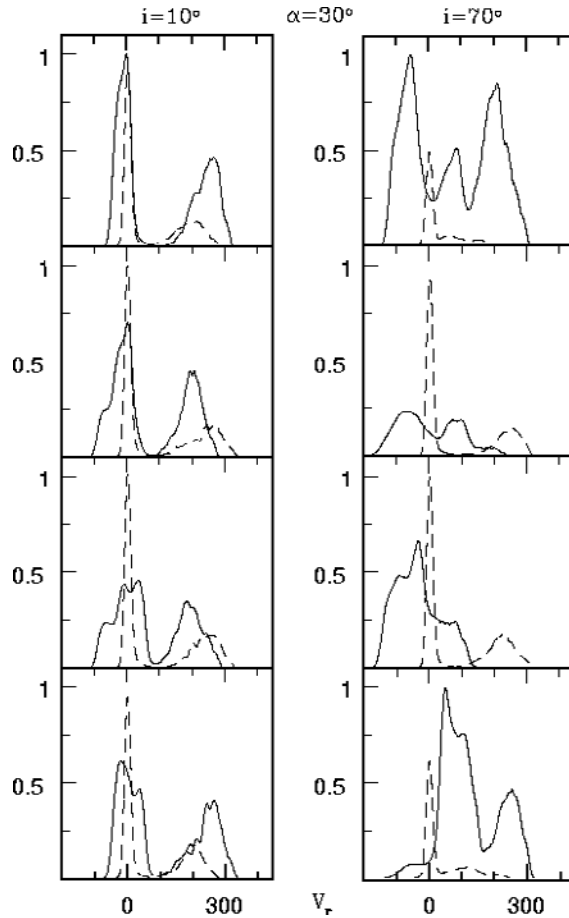


Figure 5. Theoretical profiles of the CIV 1548Å line calculated for a CTTS with a dipole magnetic field whose axis is inclined at $\alpha = 30^\circ$ to the rotation axis of the star. See text for details.

4. Conclusion

We demonstrated that the observed intensity and profiles of CIV 1550Å doublet lines significantly differ from theoretical predictions based on the assumption that the magnetic field of CTTSs near the stellar surface is close to a dipole. We conclude therefore that the geometry of CTTS magnetic field near the stellar surface is strongly non-dipolar. Multipole components of the global magnetic field of young star and/or small-scale magnetic fields in active regions probably produce a large divergence of the accreted gas stream lines within the accretion zone that presumably accounts for the disagreement between theory and observations.

Acknowledgements

We thank the SOC and the LOC of the Symposium for the invitation, financial support and hospitality.

References

Basri, G. & Bertout, C. 1989, *ApJ* 341, 340

- Calvet, N. & Gullbring, E. 1998, *ApJ* 509, 802
Gómez de Castro, A.I. & Verdugo, E. 2001, *ApJ* 548, 976
Gómez de Castro, A.I. & Verdugo, E. 2007, *ApJ* 654, 91
Kravtsova, A.S. 2003, *Astron. Lett.* 29, 463
Kravtsova, A.S., & Lamzin, S.A. 2002a, *Astron. Lett.* 28, 676
Kravtsova, A.S., & Lamzin, S.A. 2002b, *Astron. Lett.* 28, 835
Lamzin, S.A. 1995, *A&A* 295, L20
Lamzin, S.A. 1998, *Astron. Rep.* 42, 322
Lamzin, S.A. & Gomez de Castro, A.I. 1999, *Astron. Lett.* 24, 748
Lamzin, S.A. 2003a, *Astron. Rep.* 47, 498
Lamzin, S.A. 2003b, *Astron. Rep.* 47, 540
Lamzin, S.A., Kravtsova, A.S., Romanova, M.M., & Batalha, C. 2004, *Astron. Lett.* 30, 413
Romanova, M.M., Ustyugova, G.V., Koldoba, A.V., Wick, J.V., & Lovelace, R.V.E. 2003, *ApJ* 595, 1009

